Hyper-dominant species drive unexpected functional shifts in North American birds

Heng-Xing Zou[1,2*], Adam C. Smith[3,4], Yiluan Song[1,2,5], Kai Zhu[1,2], and Brian C. Weeks[2]

1. Institute for Global Change Biology, University of Michigan, Ann Arbor, MI 48109

2. School for Environment and Sustainability, University of Michigan, Ann Arbor, MI 48109

3. Department of Biology, Carleton University, Ottawa K1S 5B6, ON, Canada

4. Canadian Wildlife Service, National Wildlife Research Centre, Environment and Climate Change Canada, Ottawa K1S 5R2, ON, Canada

5. Michigan Institute for Data and AI in Society, University of Michigan, Ann Arbor, MI 48109

* Corresponding author. Email: hxzou.ecology@gmail.com

Number of words in Abstract: 189

Number of words in the main text: 3303

Number of words in Methods: 3608

Number of references: 70

Number of figures in the main text: 3

Abstract

Global environmental changes have led to widespread intraspecific shifts in functional traits across large numbers of widely distributed taxa. However, how within-species functional shifts predict community-level changes is unknown. We summarized seven key traits that are hypothesized to shift adaptively under environmental changes using local community-weighted means across North American bird communities. We find that communities shifted toward larger body mass and smaller appendage sizes over time, the opposite of widely observed within-species temporal changes in North American birds. These unexpected patterns arise from changes in the relative abundance of a very small number of hyper-dominant species, with 23 out of 470 (5%) species explaining the community-level trajectories in functional traits. These species are known to be heavily impacted—both positively and negatively—by human activities, and the idiosyncratic drivers of population sizes result in weak associations between community-level functional shifts and major bioclimatic variables but strong associations with human-induced land use changes. Our results illustrate the complexity in scaling from within-species responses to global change to community-level responses and highlight the importance of species-specific responses to the environment beyond climate when predicting functional and taxonomic diversity under global change.

Main Text

Rapid climate change has driven widespread shifts in species' abundances and distributions (1–3), as well as changes in key functional or life history traits (4, 5). Both shifts in species abundances across space and functional traits through time are expected to alter the taxonomic and functional diversity of ecological communities (6, 7). Global change drivers are often general, such as broadly consistent increases in temperature and widespread human-mediated habitat degradation (8, 9). Many of these changes could lead to similarly consistent responses among taxa; for example, as the world warms, thermoregulatory demands are likely to shift similarly across broad groups of species, driving parallel adaptations to facilitate heat dissipation (10). However, impacts of other global change factors, such as land use change, could be more idiosyncratic among species, potentially resulting in inconsistent responses (e.g., variable shifts in range (11), phenology (12), and morphology (13) across species). These inconsistencies may pose remarkable challenges for predicting how ecological communities will respond to global change from within-species responses.

Birds are a model system for relating species- and community-level responses to global change as they have comprehensive distributional (14), phylogenetic (15), behavioral (16), and functional trait (17) data, as well as long-term time series data on shifts in range, phenology, and morphology. There is reason to expect that responses to rapid environmental changes are general and directional among avian communities. Within species, shifts in key functional traits have been relatively uniform: broadly, species have become smaller (4, 18–20) and their appendages, such as beaks, tarsi, and wings,

58 have become longer (13). These shifts are often interpreted within the context of
59 thermoregulation or adaptation to more fragmented habitats and urbanization (10, 21, 22).
60 There is growing evidence that some within-species responses to climate change (e.g.,
61 range shifts) have resulted in community-level changes. Bird species have generally
62 shifted poleward and up in elevation, likely in response to the warming climate (2, 12, 23),
63 and these distributional changes are thought to have contributed to consistent local
64 changes in functional richness and evenness across large scales (7, 24, 25).
65 Should within-species changes in morphology represent consistent selection favoring
66 particular phenotypes (e.g., smaller body size) under changing climate and environments,
67 we may expect that species with that phenotype should be increasing in relative
68 abundance, shifting the community-weighted mean (CWM) of that trait in parallel with the
69 intra-specific trends. Alternatively, scaling up within-species trends to the community level
70 may be more complex. Idiosyncratic responses of individual species to the broad array of
71 environmental changes that are occurring contemporaneously may further lead to
72 inconsistencies between shared within-species responses to a single driver (e.g., climate
73 change) and community-level functional shifts (20). Relatedly, within-species changes
74 may be adaptive, but this micro-evolutionary response may not predict variation in fitness
75 among species along the same trait axis. Finally, while many within-species changes have
76 been associated with environmental change, it is unclear if these changes are adaptive or
77 the result of plasticity, in which case they may be less likely to predict shifts in fitness
78 among species. Evaluating the generality of these functional responses across the scales

is important in predicting shifts in bird community structure and ecosystem function under rapid environmental changes.

Unexpected community-level shifts in functional traits

To test if community-level functional shifts align with previous hypotheses based on within-species changes, we characterized changes in functional traits of local communities based on abundance data for 470 species spanning half a century of sampling in North America (North American Breeding Bird Survey, NABBS; Fig. 1A; (26)). To obtain robust estimates of local community composition, we aggregated abundance data within one-degree grids, aligning with the design of NABBS to have at least one route per grid with suitable access roads (see Methods). We calculated community-weighted means (CWMs) of seven key morphological and demographic traits: beak size, wing size, body mass, relative beak length, relative wing length, clutch size, and generation length. We calculated corrected beak and wing lengths (Methods); like relative beak/wing lengths, these measurements correct for the associations between beak/wing length and body mass (27). Similarly, we also corrected clutch size and generation lengths by body mass (Methods). CWMs are the average of functional trait values among species within a community, weighted by species abundances (28) and provide more mechanistic interpretations of functional shifts at the community level, more direct comparisons with within-species shifts, and are less biased by the presence of rare species than ordination-based approaches (29). To better compare with within-species expectations of functional shifts, we examined how shifts in CWMs are associated with time and environmental

variables. We considered major climatic attributes and human-induced land use changes, which have greatly affected ecological communities (9, 30, 31).

We find that community-level shifts in key morphological traits are often in opposite directions from within-species expectations based on adaptations to changing climates. CWM of body mass increases with temperature of the warmest quarter (mean = 0.168, standard error = 0.00893, $p < 0.0001$; Fig. 1C), contrary to within-species studies that have found reductions in body size as the climate has warmed over time (4, 19). The CWMs of beak and wing sizes (the first PC axes from phylogenetic PCA of four beak measurements and three wing measurements, respectively; see Methods) also positively associate with temperature (beak: 0.0354 ± 0.00177; wing: 0.0295 ± 0.00205; both $p < 0.0001$), but relative beak and wing lengths both show strongly negative associations with temperature (beak: -0.177 ± 0.00868; wing: -0.326 ± 0.0117; both $p < 0.0001$). These results contrast with within-species trends toward longer relative appendage size (4, 19, 20) that are often attributed to selection towards increased effective surface area and heat dissipation efficiency under warming (10). The CWM of clutch size positively associates with temperature (0.290 ± 0.00980, $p < 0.0001$) but negatively associates with temperature seasonality (-0.112 ± 0.00480, $p < 0.0001$; Fig. 1C). Both are contrary to within-species patterns: higher ambient temperature is associated with smaller clutch sizes often attributed to increased potential for hatching failure, and higher intra-annual fluctuations in temperature may select for larger clutch sizes as a bet-hedging strategy (32–34). Generation length represents the average age of parents in any population of a species (35, 36) and higher intra-annual fluctuations in temperature should select for earlier

reproduction (35, 37). In contrast, we observed a positive association with temperature seasonality (0.0339 ± 0.00393, $p < 0.0001$). Because temperature and precipitation seasonality only directly affect year-round residents (35), we re-analyzed the associations between climate seasonality and demographic traits separately for species that undertake long-distance seasonal migrations and those that do not according to (38). The signs of all associations are consistent among migrants and residents, but the positive association between the CWM of generation length and temperature seasonality is non-significant (fig. S1-S2).

Many studies have also suggested human-induced land use changes should favor species with certain traits, especially in urban areas where habitats are most modified (21, 22). We found that these land use changes often have stronger associations with community-level functional traits, but some of them are again contrary to expectations. The CWM of body mass is positively associated with human-modified forests and drylands (cultured land), and villages and urban areas (settlements; Fig. 1C; table S1). These results are different from the expectation that smaller body size should be favored in more human-dominated landscapes such as urban areas due to lower resource and habitat requirements (21, 22). The CWM of relative wing length is positively associated with cultured land (0.103 ± 0.00272, $p = 0.000196$) but not agricultural land and dense settlements, again different from the expectation that urban-adapted species should have larger wing-to-body ratios to assist with dispersal among fragmented habitats (21, 22). All three human-induced land use changes are negatively associated with the CWM of clutch size (agriculture: -0.272 ± 0.0277, cultured: -0.244 ± 0.0259, settlements: -0.128 ± 0.0184;

all $p < 0.0001$), contrary to the expectations that anthropogenic environmental stress should favor species with larger clutch sizes (21, 22). On the other hand, the CWM of generation length is positively associated with all three human-induced land use changes (agriculture: 0.373 ± 0.0239, cultured: 0.331 ± 0.0223, settlements: 0.395 ± 0.0157; all $p < 0.0001$). Because maximum longevity has a strongly positive correlation with generation length (35, 36), our result is therefore consistent to the expectation from previous studies that longer-lived species are favored in urban areas (21, 22).

We found that across North America, community-level shifts in morphological and demographic traits often contrast with species- and population-level expectations. We did not consider how species traits may change across space or time, which is unlikely to alter results because the magnitudes of within-species trait changes are much smaller than typical among-species variation in these traits (39). In addition to advancing our understanding of how communities have shifted through time, our findings shed new light on the interpretation of well-documented functional shifts within species. If these changes in morphological and demographic traits are adaptive to environmental changes, then it is intuitive to expect that species with traits in these more adaptive directions would increase in abundance and lead to shifts in the CWMs of the trait that are aligned with intra-specific trends. However, the shifts we find at the community level are often contrary to the shifts that have been broadly observed within species, which we interpret in three possible ways. First, observed within-species functional shifts may not be adaptive, or may not have meaningful effects on fitness (39–41). Indeed, although some morphological responses are consistent over time, whether they are indeed adaptive to environmental changes

167 remains unclear (39, 40). With more studies finding evidence both supporting and
168 opposing longstanding hypotheses based on the adaptation of climate and environmental
169 change (e.g., warming and urbanization (10, 22)), the lack of consistency on a community
170 level in our results may further indicate that within-species morphological changes may
171 not be responding to the same single driver in the environment. Second, if observed
172 intraspecific functional shifts are indeed adaptive, then our results indicate that
173 microevolutionary processes may not necessarily predict relative fitness differences
174 among species (42). Third, factors that drive adaptive intraspecific changes in functional
175 traits (e.g., climate change) may have weaker effects on relative abundance than other
176 drivers that do not drive intraspecific trait evolution but do determine differential sensitivity
177 to more significant population-level pressures (e.g., human-induced land use change;
178 (43)). As such, inconsistencies between intraspecific trait changes and shifts at the
179 community level demonstrate the complexities involved in scaling up from species to
180 community level dynamics in the context of multifaceted global environmental change.
181

182 **Nearly universal functional shifts across space**

183 Continental-scale analyses of functional shifts may mask local and regional
184 environmental factors. We explored the generality of functional shifts across local
185 communities in North America by analyzing the temporal trajectory of each local
186 community within a functional space constructed by a PCA that reduced the CWMs of the
187 seven traits into two major axes (Fig. 2A). The first PC axis (which explains 43.9% of the
188 variance) mostly represents variation in traits related to absolute body size (beak and wing

sizes and body mass); the second PC axis (which explains 16.9% of the variance) mostly reflects variation in clutch size, generation length, and relative wing length (Fig. 2A). We focus on the locations of the community in functional trait space at the start and end years (1970 and 2021), summarized by their positions in quadrants, and the overall direction (angle) of the shift for each community, summarized by the quadrant it points to (Fig. 2A).

In 1970, most local communities in central North America were characterized by larger body mass, larger absolute appendage sizes, larger clutch size, and shorter generation lengths (Fig. 2B; fig. S3). In 2021, many local communities, especially at lower latitudes, were characterized by smaller clutch sizes and longer generation lengths. Examining the directions of these shifts from 1970 to 2021, we observe an east-west divide, with local communities in the Eastern Forests and eastern parts of the Prairie regions shifting towards smaller clutch sizes and longer relative beak and wing lengths, whereas many other major avifaunal biomes in the west and north have shifted towards larger body mass and clutch sizes (Fig. 2B; fig. S4; see fig. S5 for a map of avifaunal biomes). Overall, these local-level functional shifts are broadly consistent with the results from the continent-level trends, that CWM of body mass have generally increased with time and temperature, and that clutch size and generation lengths have generally decreased with human-induced land use changes (Fig. 1C). The highly consistent community-level functional shifts that contrast with within-species expectations highlight that even when there are nearly universal changes in the environment over time that can drive consistent intraspecific functional trends among species (e.g. consistent size declines associated with increasing

210 temperatures; (4)), these conserved trends may not scale simply to analogous functional
211 shifts of local communities.
212
213 **Functional shifts driven by a few hyper-dominant species**
214 As a consequence of global environmental changes, shifts in the composition of a
215 community may emerge due to consistent changes across many of the species in a
216 community (e.g. consistent declines in the abundances of smaller species, resulting in an
217 increase in the CWM of mass through time) or extreme shifts in the abundance of a
218 relatively small number of species that either become hyper-dominant while others are
219 extirpated or decline rapidly transitioning away from being a hyper-dominant species (44).
220 To better understand the mechanisms underlying the unexpected functional shifts on the
221 community level, we quantified the contributions of each species to the temporal trends of
222 CWMs within each local community, allowing us to determine the magnitude of the
223 contributions of individual species to community-level functional shifts. For each trait, we
224 ranked the species by the number of local communities in which they contribute greatly to
225 the temporal trend (i.e., they are within the top 10% of species driving the community trend
226 in that local community). We found 4.89% of species (23 out of 470) had overwhelmingly
227 important contributions to functional shifts across North America (Fig. 3; fig. S6-S12). To
228 illustrate the importance of these top contributors to community-level functional shifts, we
229 calculated CWMs for two subcommunities: (1) only the "top contributors", and (2) the rest
230 of the species (hereafter the "standard contributors"). We then repeated all the analyses of
231 the temporal trends and environmental associations with CWMs and compared the results

232 of each subcommunity with the results derived using the full set of species (the "complete
233 communities").
234 In general, many unexpected associations between shifts in CWMs of the complete
235 communities and bioclimatic variables can be explained by the idiosyncratic responses of
236 top contributors to human-induced land use changes. Top contributors drive the
237 unexpected positive association between body mass and temperature (0.269 ± 0.0111; $p <$
238 0.0001) and negative associations between relative beak and wing lengths and
239 temperature (beak: -0.243 ± 0.00827; wing: -0.387 ± 0.0106; both $p < 0.0001$; Fig. 1C).
240 These unexpected morphological shifts can be explained by a few large-bodied species
241 that are increasingly abundant in urban, suburban, and inhabited wildlands despite
242 warming temperature, such as Canada Goose (*Branta canadensis*) and Wild Turkey
243 (*Meleagris gallopavo*; Fig. 3), and species with relatively longer beaks and wings that are
244 declining over time, such as Western Meadowlark (*Sturnella neglecta*), Horned Lark
245 (*Eremophila alpestris*), and Barn Swallow (*Hirundo rustica*). On the other hand, relative
246 beak and wing lengths of the top contributors are strongly positively associated with
247 proportions of settlements (beak: 0.287 ± 0.0165; wing: 0.0836 ± 0.0187; both $p < 0.0001$),
248 whereas these associations are strongly negative for the standard contributors (beak: -
249 0.278 ± 0.0174, $p < 0.0001$; wing: -0.0644 ± 0.0184, $p = 0.000593$; Fig. 1C). The positive
250 association for relative wing sizes may arise from the increase of long-winged songbirds,
251 such as American Robin (*Turdus migratorius*) and Red-eyed Vireo (*Vireo olivaceus*) in urban
252 areas, while the positive association for relative beak sizes may arise from the decrease of
253 small-beaked species such as House Sparrow (*Passer domesticus*; Fig. 3).

The unexpected associations between CWMs of demographic traits and climatic variables are again driven by the top contributors, as indicated by their responses to land use changes. One of the most important contributors to the CWM of clutch size is Northern Bobwhite (*Colinus virginianus*; Fig. 3), which has a large clutch size and has been declining precipitously due to habitat degradation (45), corresponding to stronger negative associations with agriculture and settlements of top contributors (agriculture: -0.305 ± 0.0297; settlements: -0.257 ± 0.0192; both $p < 0.0001$; Fig. 1C). The strongly positive associations between CWMs of generation length and agriculture and cultured lands are also driven by the top contributors (agriculture: 0.394 ± 0.0240; cultured land: 0.267 ± 0.0225; both $p < 0.0001$; Fig.1C), such as increasing abundances of Canada Goose and Northern Cardinal (*Cardinalis cardinalis*), both of which have above-average generation lengths (Fig. 3). Overall, our analyses provide strong evidence that changes in the abundance of a few hyper-dominant species have been responsible for driving the functional shifts in North American avian communities. Contrary to expectations that climatic conditions drive consistent morphological changes among species, these unexpected functional shifts on the community level are driven by the highly idiosyncratic responses of individual species as they benefit or perish because of human-induced changes in land cover and habitats (45–48).

At the continental scale, most of the unexpected functional shifts and their strong associations with human-induced land use changes can be explained by the top contributors, which are often stronger than, or even opposite to, the associations of CWMs calculated with the standard contributors. To test the generality of this result among local

276 communities, we repeated the analyses on the temporal trajectories for the top
277 contributors and standard contributors. In 1970, subcommunities composed of the top
278 contributors were mostly characterized by having larger body mass, appendage sizes, and
279 longer generation lengths (Fig. 2A-B). In 2021, subcommunities with top contributors have
280 all shifted to smaller clutch sizes and longer generation lengths (Fig. 2B; fig. S3). Strikingly,
281 spatial patterns of overall directions of functional shifts from 1970 to 2021 are nearly
282 identical between complete communities and top contributors, indicating that the top
283 contributors have driven most of the observed functional shifts of complete communities
284 (Fig. 2B). In contrast, there were no widespread shifts in functional positions within the
285 standard contributors between 1970 and 2021 (Fig. 2B; fig. S3). The uniform functional
286 shifts of top contributors are further illustrated by the temporal decrease in spatial
287 heterogeneity of functional positions (-0.000906 $\pm$ 0.000333; p = 0.00894), whereas spatial
288 heterogeneity has increased for complete communities and standard contributors
289 (complete: 0.00289 $\pm$ 0.000515, p < 0.0001; standard: 0.000605 $\pm$ 0.000267, p = 0.0279;
290 Fig. 2C; table S2). Overall, our observations emphasize the hyper-dominance of a few
291 species in driving nearly universal changes in CWMs of functional traits (49, 50), indicating
292 that environmental drivers may not induce shared responses across all species within
293 communities. Together, our results highlight the importance of considering the role of a
294 few key contributors in designing conservation and management strategies. Instead of the
295 entire community, future studies should also consider analyzing species contributions in
296 subcommunities with specific ecological roles, such as predators, herbivores, or

297 scavengers, to better understand the effect of global change on biotic interactions and
298 ecosystem functioning.
299
300 **Conclusion**
301 Rapid changes in global environments are driving within-species responses and are
302 reshaping ecological communities, but are these community-level shifts emergent
303 outcomes of general within-species processes? In North American avian communities, we
304 find significant shifts in the functional traits of communities that are not driven by
305 consistent responses among species, or by obvious climatic drivers, but instead are the
306 outcome of the idiosyncratic rise and fall of a few highly impactful species in response to
307 land use changes. These widespread, abundant, and often functionally distinctive species
308 have undergone strong changes in relative abundance, leading to local and continental
309 functional shifts that are not aligned with expectations derived from within-species trends.
310 Our evidence highlights the challenges in predicting both within-species and community-
311 level changes in functional traits from single environmental factors. On the other hand, our
312 approach provides a direction in predicting community composition by focusing on the
313 abundance and fitness of key species that contribute greatly to community structure. By
314 analyzing summary metrics such as community-weighted means of traits essential to
315 ecosystem functioning, we can further project the broader impact of species redistribution
316 and identify their key contributors. Integration of functional ecology across scales will be
317 essential to more accurately predict biotic responses to rapid global change.
318

Acknowledgements

We thank Casey Youngflesh for comments on the manuscript, and members of the Weeks and Zhu labs and IGCB Postdoc Fellows for their feedback on the project. We thank Olivia Stein for creating the illustrations used in Figure 1 and 3. We thank the numerous volunteers who collected data for the North American Breeding Bird Survey. H.-X.Z was supported by the Postdoctoral Fellowship from the Institute for Global Change Biology at the University of Michigan. Y.S. was supported by the Eric and Wendy Schmidt AI in Science Postdoctoral Fellowship, a Schmidt Sciences program. K.Z. was supported by the National Science Foundation award 2306198 and USDA McIntire-Stennis Capacity Grant award 25-PAF01509. B.C.W. was supported by the David and Lucile Packard Foundation. This research was supported in part through computational resources and services provided by the Advanced Research Computing at the University of Michigan, Ann Arbor.

Authors contributions

H.X.-Z. conceived the idea and designed the study with K.Z. and B.C.W.; H.X.-Z. curated and analyzed data with supervision from K.Z. and B.C.W. A.C.S. assisted with estimating and adjusting bird abundance; Y.S. assisted with analyzing species contributions. H.X.-Z. wrote the first draft, and all authors contributed to subsequent review and editing.

Data and materials availability

All primary data are publicly available, and all generated data will be permanently archived upon acceptance. Code is available on GitHub: https://github.com/hengxingzou/Zouetal2025bioRXiv and will be archived upon acceptance.

Methods

Species abundances and trends

We estimated species relative abundance based on data from the North American Breeding Bird Survey (NABBS), a long-term survey program started in 1966 (26). We then transformed estimates of relative abundance (relative number of individuals of a given species, compared to other times and locations; not to be confused with relative proportions of species abundance in a community) into estimates of abundance (total number of individual birds, comparable across species, locations, and times) following the methods used in previous broad-scale studies of North American bird populations (38). NABBS is a structured monitoring program that has tracked changes in bird communities across much of North America, since the late 1960s. The NABBS supplies annual estimates of population change across most of Canada and the United States for almost all terrestrial bird species (with exceptions that include some waterbirds and nocturnal species; (26)). NABBS surveys are conducted each breeding season (May, June, or July) along fixed routes of 40 km at 50 evenly spaced, independent stops. At each stop, the observer counts all identifiable birds for 3 minutes within a 400 m radius. The routes are established following secondary roads, in a random design, stratified within grid-cells of one-degree latitude and longitude. NABBS routes cover a wide range of the United States and Canada, with at least one route in most grids with suitable roads.

To estimate species relative abundances, we downloaded the 2022 release that contains survey data from 1966 to 2021 from the U.S. Geological Survey website. We consider grid cells of one degree to be “local” communities; this scale represents the

design stratification of the NABBS and is small enough that we do not expect significant variation of bioclimatic conditions within cells and large enough to contain enough survey data to estimate bird relative abundances (at least one NABBS route). To estimate relative abundances, we fit hierarchical Bayesian models with a spatial intrinsic conditional autoregressive structure using the R package *bbsBayes2* (51). To summarize, the model estimates relative abundance indices from NABBS counts on each route and year with a negative binomial distribution and weakly informative priors, and the model fitting of a species from shared information among all sites ("spatial strata"; in our case, one-by-one-degree grids). In addition, the model accounts for the spatial connection among strata by constructing a network graph, in which estimates in each stratum draw information from neighbors to estimate spatial variance and to assist in the model fitting (a "spatial smoothing" among neighbors). This spatial model not only allows for the estimation of relative abundances on a finer spatial scale but also outperforms the nonspatial counterpart in predicting population trajectories over time in poorly sampled locations (52). After accounting for spatial and temporal autocorrelation and variability in observation effort, the output of the model is a continuous year series of relative abundance estimates within the entire historical and current spatial range of each species. See (52) for the model structure and an expanded technical description of the model structure.

Prior to model fitting, we consolidated all records to the species level, pooling all subspecies or morphotypes and removing observations of unidentified species. The Great White Heron was combined with the Great Blue Heron (*Ardea herodias*), and the former

388 Cordilleran, Pacific-slope, and unidentified Western Flycatchers were all pooled into
389 Western Flycatcher (*Empidonax difficilis*). We excluded species with fewer than 50 records
390 in the whole NABBS dataset (across all routes and years). We also excluded the White-
391 crowned Pigeon (*Patagioenas leucocephala*), which was only recorded in one grid-cell. To
392 constrain our analyses to high-quality data, we limited the analysis to data from 1970 to
393 2021, removed regions outside of the continental United States and Canada (south of
394 25 ˚N, north of 55 ˚N, and west of 135 ˚W), and excluded local communities with fewer
395 than 10 species in all years. Finally, we excluded nocturnal and pelagic species, as
396 identified by the EltonTraits 1.0 dataset (16), because the NABBS protocol makes it poorly
397 suited for estimating relative abundances for these groups. In total, we conducted
398 analyses on 470 species in 1261 grids (Fig. 1A). We matched species taxonomy in NABBS
399 and functional trait datasets (see below) to the 2023 version of the Clements taxonomy
400 (15).
401 We used a spatially explicit, "first difference" model to estimate time series of annual
402 relative abundance (i.e., the species' local population trajectory) from the NABBS data for
403 each of these 470 species. This model has been commonly used to estimate population
404 status and trends from the NABBS data (52, 53). It estimates a species' population
405 trajectory in each grid as a series of annual differences from the previous year, sharing
406 information on the estimated annual differences in a spatially explicit way (i.e., among
407 neighboring grids using an intrinsic conditional autoregressive structure). However, we do
408 not formally compare model performance to determine the best model structure for each
409 species because: (1) model comparison via leave-one-out cross-validation requires strong

assumptions that individual observations are conditionally independent, which is unlikely with NABBS data; (2) different models may fit better for different species, making the pooling of all species relative abundances within a local community difficult; (3) previous work comparing alternative time series models with the NABBS data has shown that the estimated population trajectories are very similar among models (51, 52).

To estimate species relative abundances, we first fit the Bayesian models of all selected species with 1000 warm-up and 1000 sampling iterations, then obtained the posterior median of relative abundance indices in each year using the *bbsBayes2* R-package. The large spatial models for each species contain thousands to tens of thousands of parameters; we therefore used a less conservative convergence criterion by considering models as converged if no parameters had Rhats > 1.1 as converged. For 31 out of 470 species for which not all the parameters converged, we reran the models, using 2000 iterations as warm up and retaining the next 2000 sampling iterations, then we closely examined the model diagnostics for the few parameters that still had not converged in 10 species' models. The spatial model estimates parameters for each local community, enabling us to plot the maximum Rhat for each local community in the species' range. We found that for American Robin (*Turdus migratorius*), grid cells that included a parameter with Rhat > 1.1 were from data-sparse locations outside of our study region (north of 25˚N, south of 55˚N, and east of 135˚W), so we refit the model with only the data in our study region for 4000 sampling iterations. The rest of the species have patchy geographic distributions in some or all parts of their ranges: local communities in which species are detected are not spatially adjacent, leading to fewer neighboring

communities and, therefore, poor performance of the spatial model. For these nine species, we reran the model with an alternative approach to identifying spatial neighbors (Voronoi tessellation of the grid-centers within the species' range); this method increases the total number of neighbor relationships (i.e., broadens the definition of neighbor beyond the queen's-rule adjacency used in the default approach; (51)), increases the sharing of information among grids, and thereby improved the model fit, especially for species with more patchy distributions (51, 52).

Finally, we transformed the relative abundances from the Bayesian models for each of the 470 species into estimates of abundance (i.e., total number of birds for each species, year, and grid-cell), based on methods used in earlier analyses (38, 54) that account for variation in each species' detection probabilities during NABBS sampling protocols. The relative abundance of each species in each year and local community is multiplied by a series of adjustment factors that account for variations in detectability of different species. Briefly, distance adjustments account for the distances at which different species can be detected by visual or auditory signals, pair adjustments account for the probability that one individual of the breeding pair may be more easily detected (e.g., singing male vs. skulking female), and time-of-day adjustments account for the variation of detectability by the time of the survey among different species (54). NABBS was designed to compare abundance within species, not between species; these adjustments are therefore essential to our community-level analyses for not only improving accuracy but also making estimates between species comparable. We obtained the adjustment coefficients of 402 out of 470 species from (38). For the rest of the species, which are mostly waterbirds (34

species) and waterfowl (28 species), we followed previous methodologies to calculate the time-of-day adjustments (54). We then filled in missing distance and pair adjustments using the means for species within the same genus (if available), family, or order. Finally, we estimated distance and pair adjustments for Wood Stork (*Mycteria americana*), the only species without all the above information, by its behavioral patterns (no difference in detectability between sexes, and detectable from a long distance; (55)). In general, these methods remove the biases in observed counts among species by adjusting for the higher detectability of large, conspicuous, and soaring species such as pelicans, herons, and crows and the lower detectability of smaller songbirds and inconspicuous species such as warblers, wrens, and hummingbirds. We did not rerun the analyses by removing species with newly calculated adjustments because it would fundamentally change the community compositions. Rather, we checked the sensitivity by rerunning all analyses without adjustments for all species. Although these adjustments are necessary to accurately compare abundances among species, we have provided supplemental results for the full analysis without these adjustments (fig. S13-S15). Some of our conclusions are not qualitatively affected by these adjustments. In fact, our main conclusion that a small number of species greatly contribute to functional shifts across North America remained, because many common, large-bodied species that often have extreme values in functional traits are down-weighted by the adjustments. A complete species list with the adjustment factors used to estimate corrected abundances can be found in **Supplementary Data S1**.

Functional traits, community-weighted means, and species contributions

We obtained the following morphological traits from AVONET (17): beak length (both the tip of the beak to the culmen and the tip of the beak to the nares), beak width, beak depth, the length of the relaxed wing chord, Kipp's distance, the length from the carpal joint to the tip of the longest secondary, and body mass. We obtained data on clutch size from (56) and generation length from (36). Generation length is a composite measurement that roughly represents the average parental age (35). To obtain a holistic size metric for beak and wing while accounting for their phylogenetic correlations among species, we conducted phylogenetic principal component analyses (pPCA) separately on the four beak traits and three wing traits of the 470 species in our analyses using the R package *phytools* (57) and the dated tree from the 2023 version of Clements taxonomy (15). The first PC axes (PC1) explained 78.04% of and 86.94% of the total variance for the beak and wing traits, respectively (fig. S16). To correct for the tight correlation between beak and wing lengths, clutch size, and generation length with body mass (27, 33, 35), we conducted phylogenetic linear models for log-transformed values of each of these traits, with log-transformed body mass as the predictor variable, then extracted the residuals from each model (58). For beak and wing lengths, these residuals are considered as separate traits from beak and wing sizes, and we named them relative beak/wing lengths for the consistency with previous studies (27). Together, we calculated community-weighted means for seven functional traits: beak PC1, wing PC1, relative beak length, relative wing length, body mass, corrected clutch size, and corrected generation length.

We calculated community-weighted means (CWMs) at each year t from the relative abundance of species present in each grid (28):

$$CWM_t = \sum_{i=1}^{n} A_{i,t} x_i \text{ (1)},$$

where $A_{i,t}$ is the local relative abundance of species i at year t, calculated as the proportion of species i's relative abundance at year t over the sum of relative abundances of all species in that community and year. n is the number of species in the local community (i.e., $\sum_{i=1}^{n} A_{i,t} = 1$), and x_i is the value of the trait Q for species i. We characterized the temporal trend of CWM for each trait Q by a simple linear model:

$$CWM_{Q,t} = \beta_{0,Q} + \beta_Q t + \epsilon_{Q,t},$$

$$t = t_{original} - 1969, \text{ and}$$

$$\epsilon_{Q,t} \sim Normal\left(0, {\sigma_Q}^2\right) \text{ (2)},$$

where the estimated $\widehat{\beta_Q}$ is the temporal slope, and the transformed year is the difference between the original year and 1969, such that the first year in the data (1970) was set to 1. All t in the following models were transformed as such.

To further partition the contributions of each species to the temporal slope of CWMs, we decomposed $\widehat{\beta_Q}$ by first presenting it as the Ordinary Least Squares (OLS) solution using the variance-covariance form:

$$\widehat{\beta_Q} = \frac{Cov\left(CWM_{Q,t}, t\right)}{Var(t)} \text{ (3)}.$$

Combining Eqns. 1 and 3, $\widehat{\beta_Q}$ can be decomposed as

$$\widehat{\beta_Q} = \frac{Cov\left(CWM_{Q,t}, t\right)}{Var(t)} = \frac{Cov\left(\sum_{i=1}^{n} A_{i,t} x_i\right)}{Var(t)} = \sum_{i=1}^{n} \frac{Cov\left(A_{i,t}, t\right)}{Var(t)} x_i \text{ (4)}.$$

On the other hand, we can estimate the temporal slope of species i's relative abundance changes as:

$$A_{i,t} = \beta_{0,i} + \beta_{A_i} t + \epsilon_{i,t}, \text{ and}$$

$$\epsilon_{i,t} \sim Normal(0, \sigma_i^2) \text{ (5).}$$

Eqn. 5 can be written with the OLS solution using the variance-covariance form as well:

$$\widehat{\beta_{A_i}} = \frac{Cov(A_{i,t}, t)}{Var(t)} \text{ (6).}$$

Combining Eqns. 4 and 6, the temporal slope of the CWM of trait x is then

$$\widehat{\beta_Q} = \sum_{\mathrm{i}=1}^{\mathrm{n}} \widehat{\beta_{A_i}} x_i \text{ (7),}$$

i.e., the contribution of species i is its temporal slope times its trait value. Note that this decomposition (Eqn. 7) is mathematically exact—the temporal trend of CWM change is exactly the summation of individual species trends (see fig. S17-S18 for an example using real data from a local community).

Using this decomposition, we calculated species contributions to temporal changes in CWMs in each local community. For each trait, we first ranked the species in each local community by absolute values of their contributions, then counted the number of local communities in which a species ranked in the top 10% in that local community. We then ranked all species by this count and pooled the top 10 species for each of the seven traits, defined as the "top contributors" (fig. S6-S12). For each local community, we conducted the following analyses using three sets of species: the full set (complete community), a subcommunity containing only the species among the top contributors, and a subcommunity containing the rest of the species (standard contributors). We also recalculated CWMs for the top contributors and the standard contributors separately for further analyses. Note that no variables (CWMs, and relative abundance) were transformed or scaled in the calculation, but time was subtracted from the starting year (see Eqn. 2). However, for better visualization, we scaled all trait values to their averages

among all 470 species and used these scaled values as the x-axis of Fig. 3. We did not fit actual linear models to test for statistical significance; therefore, adjustment for multiple comparisons were not necessary. To test the sensitivity of our analyses, we conducted all analyses with the top five instead of top 10 contributor for each trait and found no qualitative changes in our main results (fig. S19-20).

Temporal shifts in the functional space

To further characterize the temporal change of local communities, we mapped the community in a grid each year in a functional space shared among all communities over years, constructed with a PCA of CWMs of the five key traits (beak PC1, wing PC1, body mass, generation length, and clutch size). We then tracked the location of each local community over time within the functional space, creating a trajectory, and characterized the community trajectory using the position of their start and end points (1970 and 2021) and the overall direction of change from 1970 to 2021. The overall direction (effective angle) was measured as the angle relative to the positive x-axis of the vector pointing from the beginning (1970) to the end (2021) of the trajectory (Fig. 3A). Finally, we constructed and analyzed trajectories from the CWMs of the two subcommunities: top contributors and standard contributors. To ensure all trajectories were comparable, we projected the subcommunities onto the PC axes of the PCA with the CWMs of the complete community so that all trajectories share the same axes. After obtaining the position of each local community in the functional space, measured in quadrants, we spatially mapped the local community each year and calculated the spatial heterogeneity by Moran's *I* statistic using

563 the *spdep* package (59). We compared the time series of spatial heterogeneity calculated
564 from the CWMs of the base community and the two subcommunities to further illustrate
565 the contribution of the top 23 species to the spatial patterns of functional shift over time.
566 To compare patterns of functional shifts across major biogeographical regions, we
567 categorized each local community into its bird conservation regions (BCRs; (60)). For
568 spatial grids that fall into multiple BCRs, we calculated the percentage area in each BCR
569 and only considered the one with the highest percentage. We further generalized the BCRs
570 in the continental U.S. and Canada into seven major "avifaunal biomes" (61): Arctic,
571 Northern Forest, Pacific, Intermountain West, Southwest, Prairie, and Eastern (fig. S5).
572
573 *Environmental data*
574 We quantified the association between shifts in CWMs and changes in key
575 environmental variables to explore the potential mechanisms of community-level
576 functional shifts and to facilitate their comparisons with within-species expectations. We
577 obtained a time series of the mean temperature and precipitation in the warmest quarter
578 of the year ($bio10$ and $bio18$) from the WorldClim2 dataset (62). The warmest quarter
579 coincides with both the breeding season of most North American birds and the period
580 when NABBS is conducted. Both $bio10$ and $bio18$ are strongly correlated with mean
581 annual temperature (MAT; linear model, slope = 0.650, 95% CI = [0.649, 0.651], $p < 0.0001$)
582 and mean annual precipitation (MAP; slope = 0.173, 95% CI = [0.172, 0.174], $p < 0.0001$);
583 therefore, we do not expect results to be qualitatively different if using MAT and MAP
584 instead. To evaluate the effect of seasonality on key demographic traits, we calculated the

seasonality of temperature and precipitation as the difference between the warmest and coldest months ($bio5 - bio6$) and the wettest and driest months ($bio13 - bio14$; (63)). To explore the relationship between human-induced land use change and functional shifts, we obtained land cover data from the HYDE 3.3 database, which estimates historical anthropogenic land use changes (64). The HYDE data contain 20 categories of anthropogenic biomes, or "anthromes" (9, 30); we generalized land use types into four main categories: settlements, which contains urban areas and villages; agriculture, which contains croplands and rangelands; cultured land, which contains woodland and drylands with human inhabitants, and wild land. Settlements and agriculture are intensely impacted by human activities, cultured land receives less human impact, and wildland contains woodland and drylands with minimum human impacts. To match the spatial resolution of estimated species abundances, we calculated the proportions of areas in each land use category in a one-degree latitude and longitude grid cell. We obtained yearly time series of all the above environmental data from 1970 to 2021 and aggregated them to the same one-degree grid cells as our abundance data.

Model fitting

Before fitting the full model, we first fit the following linear mixed-effect models with the R package *lme4* (65):

$$CWM_Q = \beta_{0,Q} + \beta_{1,Q}t + b_{g,Q} + \epsilon_Q,$$

$$b_{g,Q} \sim Normal\left(0, \sigma_g^2\right), \text{ and}$$

$$\epsilon_Q \sim Normal(0, \sigma^2) \text{ (8).}$$

Specifically, we separately modeled the CWM of each trait Q as a linear response of transformed year t with slope $\beta_{1,Q}$, intercept $\beta_{0,Q}$, grid-level random effect $b_{g,Q}$, and the overall residual ϵ_Q. We used a simple grid-level random effect because there was no spatial autocorrelation in the residuals of the full model (see below). Both $b_{g,Q}$ and ϵ_Q are normally distributed. We weighted the fitted residual $\widehat{\epsilon_Q}$ by the inverse of the overall abundance of the local community within each grid. This weighting corrects for the potentially higher measurement errors in communities with lower overall abundance. In all linear mixed effects models, we log-transformed the CWM of body mass. Because we fit the CWM of each trait separately, we adjusted the p-value of the models using the Benjamini-Hochberg method (66). Fitting the year-only model yielded significant slopes for CWMs of all traits but generation length (table S3).

Then, to explore whether the year effect still accounted for variances unexplained by all environmental variables (bioclimatic variables and human-induced land use proportions), we fit a year-environment model:

$$CWM_Q = \beta_{0,Q} + \beta_{1,Q}t + E\beta_{2,Q} + b_{g,Q} + \epsilon_Q \quad (9),$$

where E is a vector of environmental variables, $\beta_{2,Q}$ is a vector of slopes corresponding to each environmental variable, and $b_{g,Q}$ and ϵ_Q follow definitions in Eqn. 8. Because the land use type is proportional data (summing to 1), we removed wild land when fitting the model. We then scaled all the environmental variables to ensure the slopes are comparable in magnitude. In this model, year slopes for CWMs of all traits were significant and had the same signs comparing to the year-only model (**Supplementary Data S3**), indicating that year explained variations in CWMs of most traits even after accounting for all

environmental variables, which changed temporally, and should be considered as a fixed effect rather than a temporal random effect.

Finally, we fit the full model with year, environmental variables, year-environment interactions, and grid-level random effects:

$$CWM_Q = \beta_{0,Q} + \beta_{1,Q}t + E\beta_{2,Q} + (t \times E)\beta_{3,Q} + b_{g,Q} + \epsilon_Q \quad (10),$$

where $t \times E$ denotes the interactive effects between year and environmental variables. We analyzed the models of each CWM using variograms in the R package *gstat* (67) and found no evidence of strong spatial autocorrelation in the residuals (fig. S21). We then fit the full model (Eqn. 10) with CWMs of the two subcommunities, consisting of the top contributors and the standard contributors, then compared their slopes of the same predictor variables. We fit separate models rather than using group-level slopes within a single model because CWMs do not contain species identities and therefore can only be calculated for different groups of species. See **Supplementary Data S4** for full diagnostics of the models.

Temperature and precipitation seasonality may only affect the life history strategies of residents who are exposed to climatic extremes throughout the whole year. Therefore, we analyzed the associations between temperature/precipitation seasonality and the two demographic traits, clutch size and generation length, separately for residents and migrants. To do so, we filtered species by their migration status according to (38), then separately calculated the CWMs for each group in local communities.

Software

All analyses were conducted by R version 4.4.1. (68). In addition to specific packages mentioned in methods, all data wrangling and visualization were conducted using the package *tidyverse* (69), and all geospatial analyses were conducted using the package *sf* (70).

Reference

1. C. Parmesan, *et al.*, Poleward shifts in geographical ranges of butterfly species associated with regional warming. *Nature* **399**, 579–583 (1999).

2. M. W. Tingley, W. B. Monahan, S. R. Beissinger, C. Moritz, Birds track their Grinnellian niche through a century of climate change. *Proceedings of the National Academy of Sciences of the United States of America* **106**, 19637–19643 (2009).

3. I.-C. Chen, J. K. Hill, R. Ohlemüller, D. B. Roy, C. D. Thomas, Rapid Range Shifts of Species Associated with High Levels of Climate Warming. *Science* **333**, 1024–1026 (2011).

4. B. C. Weeks, *et al.*, Shared morphological consequences of global warming in North American migratory birds. *Ecology Letters* **23**, 316–325 (2020).

5. S. A. MacLean, S. R. Beissinger, Species' traits as predictors of range shifts under contemporary climate change: A review and meta-analysis. *Global Change Biology* **23**, 4094–4105 (2017).

6. K. Zhu, *et al.*, Rapid shifts in grassland communities driven by climate change. *Nat Ecol Evol* **8**, 2252–2264 (2024).

7. M. A. Jarzyna, W. Jetz, A near half-century of temporal change in different facets of avian diversity. *Global Change Biology* **23**, 2999–3011 (2017).

8. J. Rogelj, M. Meinshausen, R. Knutti, Global warming under old and new scenarios using IPCC climate sensitivity range estimates. *Nature Clim Change* **2**, 248–253 (2012).

9. E. C. Ellis, K. Klein Goldewijk, S. Siebert, D. Lightman, N. Ramankutty, Anthropogenic transformation of the biomes, 1700 to 2000. *Global Ecology and Biogeography* **19**, 589–606 (2010).

10. S. Ryding, M. Klaassen, G. J. Tattersall, J. L. Gardner, M. R. E. Symonds, Shape-shifting: changing animal morphologies as a response to climatic warming. *Trends in Ecology & Evolution* **36**, 1036–1048 (2021).

11. C. Moritz, *et al.*, Impact of a century of climate change on small-mammal communities in Yosemite National Park, USA. *Science* **322**, 261–264 (2008).

12. M. H. C. Neate-Clegg, B. A. Tonelli, M. W. Tingley, Advances in breeding phenology outpace latitudinal and elevational shifts for North American birds tracking temperature. *Nat Ecol Evol* 1–10 (2024). https://doi.org/10.1038/s41559-024-02536-z.

13. S. Ryding, A. McQueen, M. Klaassen, G. J. Tattersall, M. R. E. Symonds, Long- and short-term responses to climate change in body and appendage size of diverse Australian birds. *Global Change Biology* **30**, e17517 (2024).

14. D. W. Gibbons, P. F. Donald, H.-G. Bauer, L. Fornasari, I. K. Dawson, Mapping avian distributions: the evolution of bird atlases. *Bird Study* **54**, 324–334 (2007).

15. E. J. McTavish, *et al.*, A complete and dynamic tree of birds. *Proceedings of the National Academy of Sciences* **122**, e2409658122 (2025).

16. H. Wilman, *et al.*, EltonTraits 1.0: Species-level foraging attributes of the world's birds and mammals. *Ecology* **95**, 2027–2027 (2014).

17. J. A. Tobias, *et al.*, AVONET: morphological, ecological and geographical data for all birds. *Ecology Letters* **25**, 581–597 (2022).

18. J. A. Sheridan, D. Bickford, Shrinking body size as an ecological response to climate change. *Nature Clim Change* **1**, 401–406 (2011).

19. V. Jirinec, *et al.*, Morphological consequences of climate change for resident birds in intact Amazonian rainforest. *Science Advances* **7**, eabk1743 (2021).

20. C. Youngflesh, J. F. Saracco, R. B. Siegel, M. W. Tingley, Abiotic conditions shape spatial and temporal morphological variation in North American birds. *Nat Ecol Evol* **6**, 1860–1870 (2022).

21. A. P. Møller, Successful city dwellers: a comparative study of the ecological characteristics of urban birds in the Western Palearctic. *Oecologia* **159**, 849–858 (2009).

22. M. H. C. Neate-Clegg, *et al.*, Traits shaping urban tolerance in birds differ around the world. *Current Biology* **33**, 1677-1688.e6 (2023).

23. C. S. Rushing, J. A. Royle, D. J. Ziolkowski, K. L. Pardieck, Migratory behavior and winter geography drive differential range shifts of eastern birds in response to recent climate change. *Proceedings of the National Academy of Sciences* **117**, 12897–12903 (2020).

24. A. M. Schipper, *et al.*, Contrasting changes in the abundance and diversity of North American bird assemblages from 1971 to 2010. *Global Change Biology* **22**, 3948–3959 (2016).

25. J.-Y. Barnagaud, P. Gaüzère, B. Zuckerberg, K. Princé, J.-C. Svenning, Temporal changes in bird functional diversity across the United States. *Oecologia* **185**, 737–748 (2017).

26. J. R. Sauer, *et al.*, The first 50 years of the North American Breeding Bird Survey. *The Condor* **119**, 576–593 (2017).

27. S. Ryding, A. McQueen, Multiple regression, not ratios, for analyzing relative appendage size. *Evol Ecol* (2025). https://doi.org/10.1007/s10682-025-10346-3.

28. S. Lavorel, *et al.*, Assessing functional diversity in the field – methodology matters! *Functional Ecology* **22**, 134–147 (2008).

29. S. Villéger, N. W. H. Mason, D. Mouillot, New Multidimensional Functional Diversity Indices for a Multifaceted Framework in Functional Ecology. *Ecology* **89**, 2290–2301 (2008).

30. E. C. Ellis, *et al.*, People have shaped most of terrestrial nature for at least 12,000 years. *Proceedings of the National Academy of Sciences* **118**, e2023483118 (2021).

31. K. L. Thompson, J. M. Chase, R. Remelgado, C. Meyer, The interacting effects of climate and land-cover change on bird communities in the United States. *Ecography* **2025**, e07949 (2025).

32. R. E. Ricklefs, Geographical Variation in Clutch Size among Passerine Birds: Ashmole's Hypothesis. *The Auk* **97**, 38–49 (1980).

33. W. Jetz, C. H. Sekercioglu, K. Böhning-Gaese, The Worldwide Variation in Avian Clutch Size across Species and Space. *PLOS Biology* **6**, e303 (2008).

34. C. B. Cooper, W. M. Hochachka, G. Butcher, A. A. Dhondt, Seasonal and Latitudinal Trends in Clutch Size: Thermal Constraints During Laying and Incubation. *Ecology* **86**, 2018–2031 (2005).

35. C. Youngflesh, *et al.*, Environmental Variability Shapes Life History of the World's Birds. *Ecology Letters* **28**, e70077 (2025).

36. J. P. Bird, *et al.*, Generation lengths of the world's birds and their implications for extinction risk. *Conservation Biology* **34**, 1252–1261 (2020).

37. W. M. Schaffer, Optimal Reproductive Effort in Fluctuating Environments. *The American Naturalist* **108**, 783–790 (1974).

38. K. V. Rosenberg, *et al.*, Decline of the North American avifauna. *Science* **366**, 120–124 (2019).

39. A. Nord, E. Persson, J. K. R. Tabh, E. Thoral, Shrinking body size may not provide meaningful thermoregulatory benefits in a warmer world. *Nat Ecol Evol* **8**, 387–389 (2024).

40. J. K. R. Tabh, *et al.*, Limited evidence that body size shrinking and shape-shifting alleviate thermoregulatory pressures in a warmer world. *Commun Biol* **8**, 1–13 (2025).

41. C. Teplitsky, J. A. Mills, J. S. Alho, J. W. Yarrall, J. Merilä, Bergmann's rule and climate change revisited: Disentangling environmental and genetic responses in a wild bird population. *Proceedings of the National Academy of Sciences* **105**, 13492–13496 (2008).

42. C. P. terHorst, *et al.*, Evolution in a Community Context: Trait Responses to Multiple Species Interactions. *The American Naturalist* **191**, 368–380 (2018).

43. T. Dias, *et al.*, Long-term increases in wing length occur independently of changes in climate and climate-driven shifts in body size. *Proceedings of the Royal Society B: Biological Sciences* **292**, 20242556 (2025).

44. C. H. Trisos, C. Merow, A. L. Pigot, The projected timing of abrupt ecological disruption from climate change. *Nature* **580**, 496–501 (2020).

45. F. Hernández, L. A. Brennan, S. J. DeMaso, J. P. Sands, D. B. Wester, On reversing the northern bobwhite population decline: 20 years later. *Wildlife Society Bulletin* **37**, 177–188 (2013).

46. J. R. Allan, J. S. Kirby, C. J. Feare, The biology of canada geese Branta canadensis in relation to the management of feral populations. *Wildlife Biology* **1**, 129–143 (1995).

47. J. L. Tapley, R. K. Abernethy, J. E. Kennamer, N. Carolina, Status and distribution of the wild turkey in 2004 in *Proceedings of the National Wild Turkey Symposium*, (2005), pp. 21–32.

48. I. Benmazouz, *et al.*, Corvids in Urban Environments: A Systematic Global Literature Review. *Animals* **11**, 3226 (2021).

49. K. Princé, B. Zuckerberg, Climate change in our backyards: the reshuffling of North America's winter bird communities. *Global Change Biology* **21**, 572–585 (2015).

50. G. J. Di Cecco, A. H. Hurlbert, Anthropogenic drivers of avian community turnover from local to regional scales. *Global Change Biology* **28**, 770–781 (2022).

51. B. P. M. Edwards, A. C. Smith, S. LaZerte, bbsBayes2: Hierarchical Bayesian Analysis of North American BBS Data. (2023). Deposited 2023.

52. A. C. Smith, *et al.*, Spatially explicit Bayesian hierarchical models improve estimates of avian population status and trends. *Ornithological Applications* **126**, duad056 (2024).

53. W. A. Link, J. R. Sauer, D. K. Niven, Model selection for the North American Breeding Bird Survey: A comparison of methods. *The Condor* **119**, 546–556 (2017).

54. J. Stanton, P. Blancher, K. Rosenberg, A. Panjabi, W. Thogmartin, Estimating uncertainty of North American landbird population sizes. *Avian Conservation and Ecology* **14** (2019).

55. M. C. Coulter, J. A. Rodgers Jr., J. C. Ogden, F. C. Depkin, Wood Stork (Mycteria americana), version 1.0. *Birds of the World* (2020). https://doi.org/10.2173/bow.woosto.01species_shared.bow.project_name.

56. N. P. Myhrvold, *et al.*, An amniote life-history database to perform comparative analyses with birds, mammals, and reptiles. *Ecology* **96**, 3109–3109 (2015).

57. L. J. Revell, phytools 2.0: an updated R ecosystem for phylogenetic comparative methods (and other things). *PeerJ* **12**, e16505 (2024).

58. Y. Xu, *et al.*, Ecological predictors of interspecific variation in bird bill and leg lengths on a global scale. *Proceedings of the Royal Society B: Biological Sciences* **290**, 20231387 (2023).

59. R. Bivand, R Packages for Analyzing Spatial Data: A Comparative Case Study with Areal Data. *Geographical Analysis* **54**, 488–518 (2022).

60. J. R. Sauer, J. E. Fallon, R. Johnson, Use of North American Breeding Bird Survey Data to Estimate Population Change for Bird Conservation Regions. *The Journal of Wildlife Management* **67**, 372–389 (2003).

61. T. L. Crewe, J. D. McCracken, P. D. Taylor, D. Lepage, A. E. Heagy, The Canadian Migration Monitoring Network-Réseau canadien de surveillance des migrations: Ten-year report on monitoring landbird population change. *CMMN-RCSM Scientific Technical Report* **1** (2008).

62. S. E. Fick, R. J. Hijmans, WorldClim 2: new 1-km spatial resolution climate surfaces for global land areas. *International Journal of Climatology* **37**, 4302–4315 (2017).

63. A. J. Boyce, B. G. Freeman, A. E. Mitchell, T. E. Martin, Clutch size declines with elevation in tropical birds. *The Auk* **132**, 424–432 (2015).

64. C. G. M. K. Goldewijk, Anthropogenic land-use estimates for the Holocene; HYDE 3.2. DANS Data Station Archaeology. https://doi.org/10.17026/dans-25g-gez3. Deposited 29 September 2017.

65. D. Bates, M. Mächler, B. Bolker, S. Walker, Fitting Linear Mixed-Effects Models Using lme4. *Journal of Statistical Software* **67**, 1–48 (2015).

66. Y. Benjamini, Y. Hochberg, Controlling the False Discovery Rate: A Practical and Powerful Approach to Multiple Testing. *Journal of the Royal Statistical Society: Series B (Methodological)* **57**, 289–300 (1995).

67. E. J. Pebesma, Multivariable geostatistics in S: the gstat package. *Computers & Geosciences* **30**, 683–691 (2004).

68. R Core Team, R: A language and environment for statistical computing. (2024).

69. H. Wickham, *et al.*, Welcome to the Tidyverse. *Journal of Open Source Software* **4**, 1686 (2019).

70. E. Pebesma, Simple Features for R: Standardized Support for Spatial Vector Data. *The R Journal* (2018).

Figure Legends

Fig. 1: Overview of the analyses and associations between functional shifts and environmental variables. **A.** Map of the study region, showing the 1261 local communities (one by one degree grids) included in the analyses. **B.** Overview of the analyses. **C.** Associations between community-weighted means (CWMs) of seven key functional traits and main environmental variables, including climate, human-induced land use, and year. CWMs are calculated from either all species in the communities (complete communities), only the top contributors, or only the rest of the species (standard contributors). All statistics are shown in table S1. Illustration by Olivia Stein.

Fig. 2: Analyzing the temporal trajectory of local communities in the functional space. **A.** The functional space constructed by PCA of all communities by their community-weighted mean measurements over time, and a temporal trajectory of one local community (40˚N, 110˚W) moving through the functional space over time, showing the start and end points and the overall direction (effective angle). In the trajectory, lighter shades represent earlier years, and darker shades represent later years. The two panels represent the same functional space, but the scales are adjusted for better visualization. **B.** Maps of each local community's start and end positions in the functional space, measured by the quadrants in **A**, and the overall direction of the functional shifts, measured by the quadrants to which the trajectory travels. Columns show results for complete communities, subcommunities with top contributors, and subcommunities with the standard contributors. **C.** Spatial heterogeneity of functional positions of the base communities, top contributors, and the rest of the species, calculated as Moran's *I* from the maps. A Moran's *I* closer to 0 means lower spatial heterogeneity.

Fig. 3: Species contributions to the community-weighted means (CWMs) of seven key functional traits. Panels only include species that contribute substantially (ranked top 10% of all species in a local community) in at least one local community; point size denotes the number of grids in which a species contributes greatly. The sign of the contribution depends on the species' temporal trends of relative abundance and its trait value, e.g., if a species with below-average trait value increases in relative abundance, it will contribute negatively by lowering the CWM of the trait. For each trait, the identity of the top 10 species that contribute to the CWMs of the most local communities is labeled; pooling all these species results in 25 top contributors of the observed functional shifts over time, shown on the right. For each panel, the x-axis is the scaled trait values, and the y-axis is the median of the temporal slopes of relative abundances across each species' range. Shades denote the absolute magnitudes of species contributions: colder colors represent negative contributions, and warmer colors represent positive contributions. Axes and scales are different for each panel for better visualization. Illustrations by Olivia Stein.

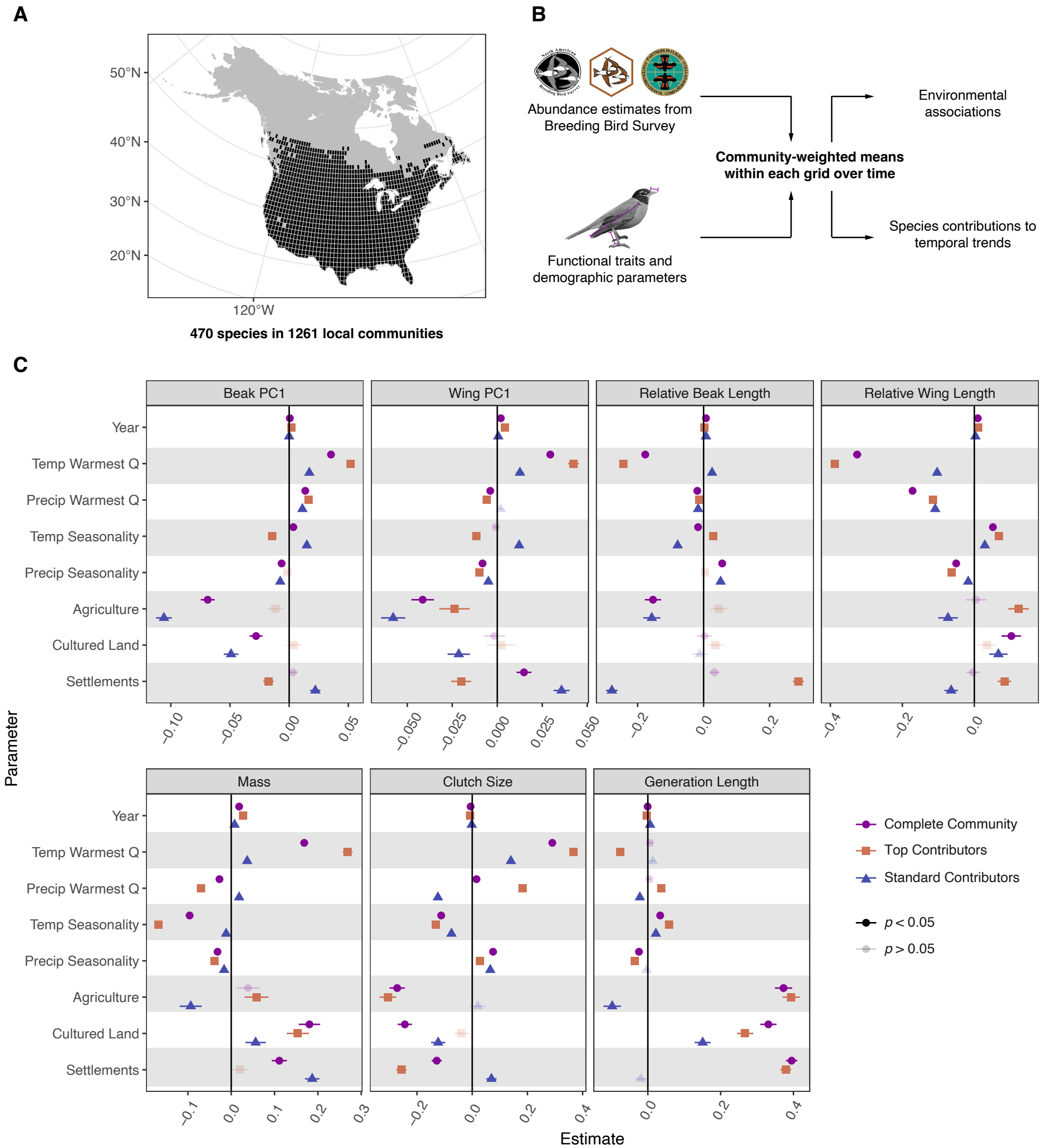
A
50°N
40°N
30°N
20°N
120°W
470 species in 1261 local communities
B
Abundance estimates from Breeding Bird Survey
Functional traits and demographic parameters
Community-weighted means within each grid over time
Environmental associations
Species contributions to temporal trends
C
Beak PC1
Wing PC1
Relative Beak Length
Relative Wing Length
Mass
Clutch Size
Generation Length
Year
Temp Warmest Q
Precip Warmest Q
Temp Seasonality
Precip Seasonality
Agriculture
Cultured Land
Settlements
Parameter
Estimate
Complete Community
Top Contributors
Standard Contributors
p < 0.05
p > 0.05

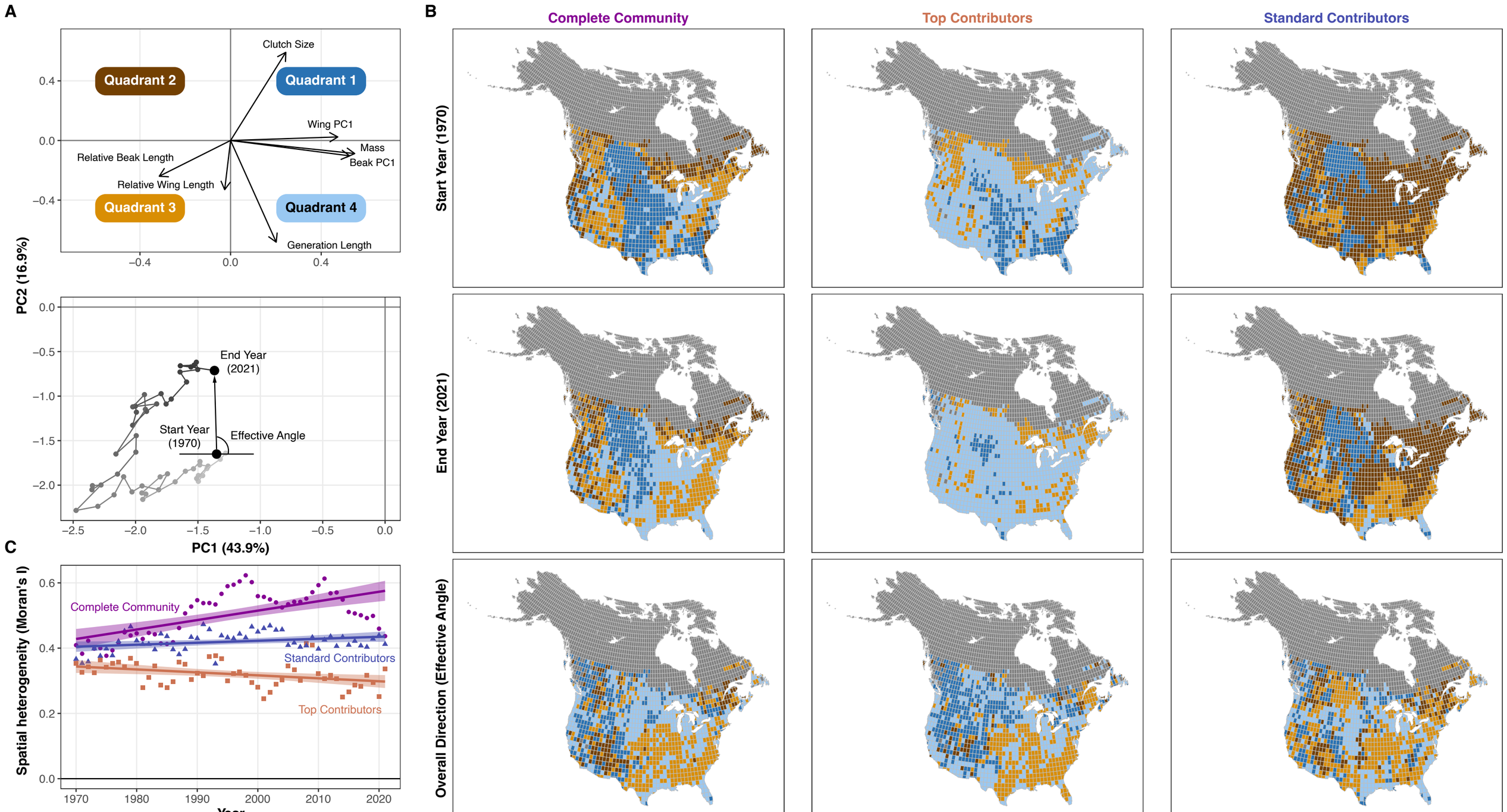
A
Clutch Size
Quadrant 2
Quadrant 1
Wing PC1
Mass
Beak PC1
Relative Beak Length
Relative Wing Length
Quadrant 3
Quadrant 4
Generation Length
PC2 (16.9%)
End Year
(2021)
Start Year
(1970)
Effective Angle
PC1 (43.9%)
B
Complete Community
Top Contributors
Standard Contributors
Start Year (1970)
End Year (2021)
Overall Direction (Effective Angle)
C
Spatial heterogeneity (Moran's I)
Complete Community
Standard Contributors
Top Contributors
Year

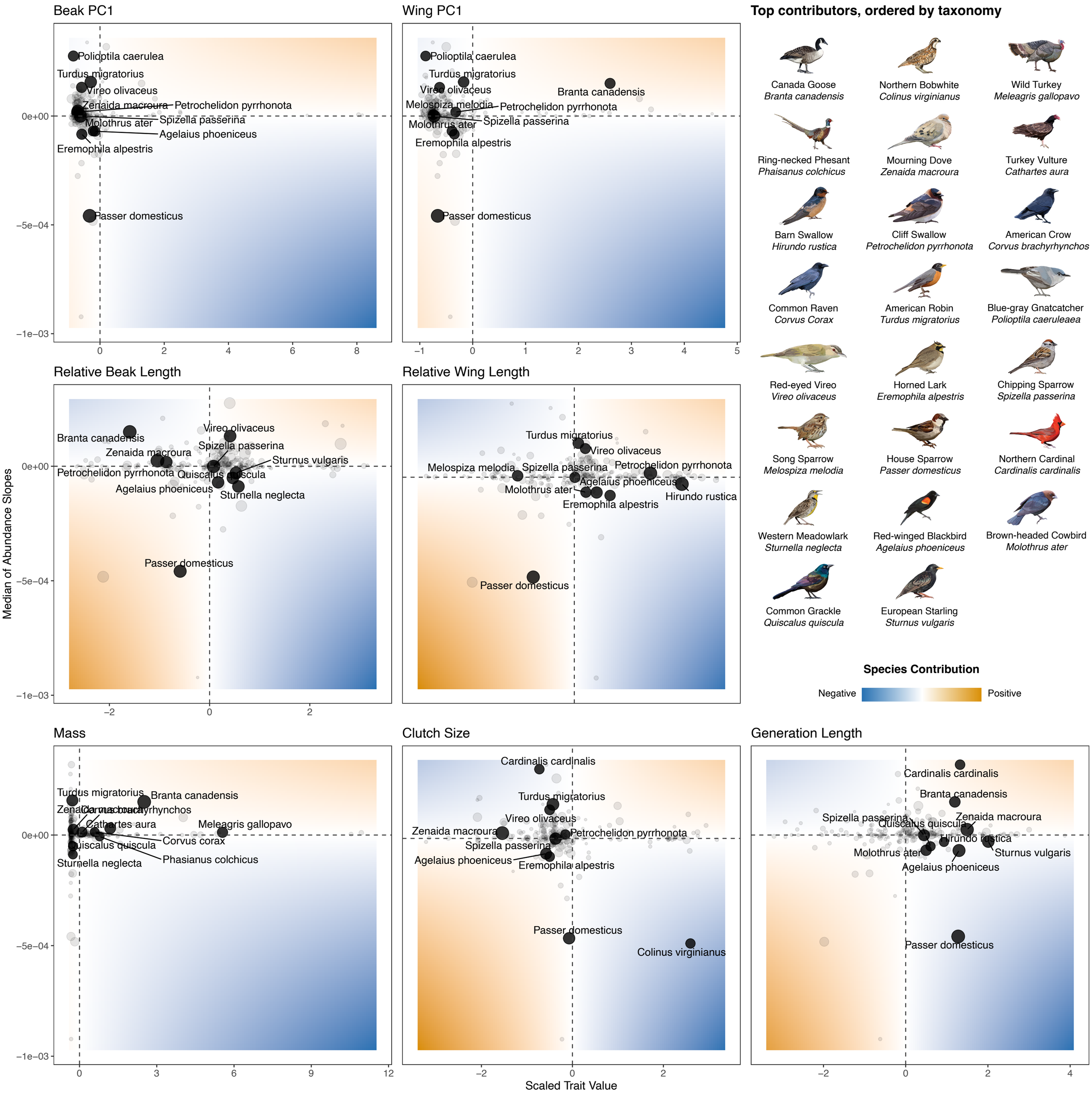
Beak PC1
Polioptila caerulea
Turdus migratorius
Vireo olivaceus
Zenaida macroura
Petrochelidon pyrrhonota
Molothrus ater
Spizella passerina
Agelaius phoeniceus
Eremophila alpestris
Passer domesticus
Wing PC1
Polioptila caerulea
Turdus migratorius
Vireo olivaceus
Branta canadensis
Melospiza melodia
Petrochelidon pyrrhonota
Molothrus ater
Spizella passerina
Eremophila alpestris
Passer domesticus
Relative Beak Length
Branta canadensis
Vireo olivaceus
Zenaida macroura
Spizella passerina
Sturnus vulgaris
Petrochelidon pyrrhonota
Quiscalus quiscula
Agelaius phoeniceus
Sturnella neglecta
Passer domesticus
Relative Wing Length
Turdus migratorius
Vireo olivaceus
Melospiza melodia
Spizella passerina
Petrochelidon pyrrhonota
Agelaius phoeniceus
Molothrus ater
Hirundo rustica
Eremophila alpestris
Passer domesticus
Median of Abundance Slopes
0e+00
−5e−04
−1e−03
Top contributors, ordered by taxonomy
Canada Goose
Branta canadensis
Northern Bobwhite
Colinus virginianus
Wild Turkey
Meleagris gallopavo
Ring-necked Phesant
Phaisanus colchicus
Mourning Dove
Zenaida macroura
Turkey Vulture
Cathartes aura
Barn Swallow
Hirundo rustica
Cliff Swallow
Petrochelidon pyrrhonota
American Crow
Corvus brachyrhynchos
Common Raven
Corvus Corax
American Robin
Turdus migratorius
Blue-gray Gnatcatcher
Polioptila caeruleaea
Red-eyed Vireo
Vireo olivaceus
Horned Lark
Eremophila alpestris
Chipping Sparrow
Spizella passerina
Song Sparrow
Melospiza melodia
House Sparrow
Passer domesticus
Northern Cardinal
Cardinalis cardinalis
Western Meadowlark
Sturnella neglecta
Red-winged Blackbird
Agelaius phoeniceus
Brown-headed Cowbird
Molothrus ater
Common Grackle
Quiscalus quiscula
European Starling
Sturnus vulgaris
Species Contribution
Negative
Positive
Mass
Turdus migratorius
Branta canadensis
Zenaida macroura
Corvus brachyrhynchos
Cathartes aura
Meleagris gallopavo
Corvus corax
Quiscalus quiscula
Phasianus colchicus
Sturnella neglecta
Clutch Size
Cardinalis cardinalis
Turdus migratorius
Vireo olivaceus
Zenaida macroura
Petrochelidon pyrrhonota
Spizella passerina
Agelaius phoeniceus
Eremophila alpestris
Passer domesticus
Colinus virginianus
Generation Length
Cardinalis cardinalis
Branta canadensis
Spizella passerina
Zenaida macroura
Quiscalus quiscula
Hirundo rustica
Molothrus ater
Sturnus vulgaris
Agelaius phoeniceus
Passer domesticus
Scaled Trait Value